

# IBA of ZrO<sub>2</sub>:Yb/Si thin films produced by the spray pyrolysis method

E. Andrade<sup>a,\*</sup>, E.B. Ramirez<sup>b</sup>, J.C. Alonso<sup>b</sup>, M.F. Rocha<sup>c</sup>

<sup>a</sup> Instituto de Física, Universidad Nacional Autónoma de México, Apartado Postal 20-364, 01000 México, México

<sup>b</sup> Instituto de Investigaciones en Materiales, UNAM, Ciudad Universitaria, A.P. 70-360, México D.F. 04510, México

<sup>c</sup> Escuela Superior de Ingeniería Mecánica y Eléctrica, IPN, C.P., México D.F. 07738, México

Available online 18 March 2008

## Abstract

A spray pyrolysis method was used to produce thin films of ZrO<sub>2</sub> doped with different Yb concentrations on Si(100). The films of these ionic semiconductors have potential applications as solid electrolytes in modern ceramic fuel cells of second generation. The determination of the atomic composition of the films is very important because it strongly affects the chemical and thermal stability, as well as electrical properties of the films. A combination of two Ion Beam Analysis (IBA) methods was applied to obtain the atomic composition of the films. A nuclear reaction analysis (NRA) method using a low energy deuterium beam was applied to measure the oxygen content of the films. Heavy ion Rutherford backscattering (HI-RBS) method using a <sup>12</sup>C<sup>3+</sup> beam was applied to measure the Yb and Zr atomic profiles of the samples. X-ray diffraction (XRD) and ellipsometry were also employed to determine structural properties and refractive index of the films, respectively. The IBA, XRD and the ellipsometry supply a wide range of information about the film layers, which can be used for qualification as well as for feedback to the films production.

© 2008 Published by Elsevier B.V.

PACS: 61.10.Eq; 61.10.Ez; 61.66.f

Keywords: YbSZ films; Ultrasonic spray pyrolysis; XRD; Ionic conductivity

## 1. Introduction

The preparation of thin films of solid oxide electrolytes by different techniques has become very important for second-generation solid oxide fuel cells (SOFCs) [1–3]. Due to its high ionic conductivity at high temperatures and chemical stability in both oxidizing and reducing atmospheres, yttria stabilized zirconia (YSZ) has been the most widely studied material as solid oxide electrolyte for SOFCs. However, other rare earth elements (Yb, Ce, Gd, etc), has also been investigated as zirconia dopants for such applications [1–3]. A number of studies have shown that the ionic conductivity of stabilized zirconia, which is attributed to the mobility of oxygen vacancies created by the stabilizer dopant, is maximum for a certain dopant level (typically 8–20%) and that it tends to be highest as the ionic

radius of the dopant closely matches that of Zr<sup>+4</sup> host cation [3,4]. Tablets and/or bars prepared from compactation and sintering of fine grained powders of stabilized zirconia with ytterbia (YbSZ) have been reported to have a conductivity higher than that of YSZ [2,5]. However, to our knowledge, there are scarce reports on the preparation, composition and structure of YbSZ thin films [6].

In this work, we report the preparation of YbSZ thin films with different content of Yb, by the spray pyrolysis method. The atomic composition of the YbSZ films was measured using IBA methods. There are different IBA methods able to provide the film stoichiometry of the Yb and Zr oxides. We selected a combination of two IBA methods as the most favorable: (a) a RBS/NRA method using a low energy deuterium beam was applied to obtain the oxygen concentration through nuclear reactions (NR) produced on oxygen nuclei. This method lacks good mass separation and has a poor depth resolution; (b) a HI-RBS method using a <sup>12</sup>C<sup>3+</sup> was applied to measure the

\* Corresponding author. Tel.: +52 55 5622 5055; fax: +52 55 5622 5046.  
E-mail address: [andrade@fisica.unam.mx](mailto:andrade@fisica.unam.mx) (E. Andrade).

Zr and Yb concentration profiles. This method has a good mass separation and excellent depth profile resolution. Other complementary material analysis techniques used were XRD and ellipsometry in order to obtain the crystallographic properties and ellipsometry to measure the refractive index and thickness of the films, respectively.

## 2. Experimental details

The YbSZ films were deposited by the ultrasonic spray pyrolysis method, which has been used recently for the preparation of pure zirconia ( $\text{ZrO}_2$ ) and YSZ thin films [7,8]. The substrates used to deposit the films were single crystalline silicon (100) n-type, 0.1–2.0  $\Omega$  cm. The precursor solution was prepared by dissolving a fixed amount (0.025 M) of zirconium (IV) acetylacetonate [ $\text{Zr}(\text{acac})_4 = \text{Zr}(\text{C}_5\text{H}_7\text{O}_2)_4$ ] from Sigma-Aldrich Chemicals, in anhydrous methanol. The dopant level of  $\text{Yb}_2\text{O}_3$  was controlled by adding different concentrations of ytterbium acetate hydrate [ $\text{Y}(\text{acet})_3(\text{H}_2\text{O})_x = \text{Yb}(\text{C}_2\text{H}_3\text{O}_2)_3(\text{H}_2\text{O})_x$ ] (also from Sigma-Aldrich), to the precursor solution. The molar concentration of  $\text{Yb}(\text{acet})_3(\text{H}_2\text{O})_x$  were 0.0025 M (YbSZ1), 0.005 M (YbSZ2), 0.0075 M (YbSZ3) and 0.01 M (YbSZ4). The substrate temperature ( $T_s$ ) was kept constant at 425 °C, air gas carrier was used as and director gas flow rates, were fixed at 3.5 l/min and 1.5 l/min, respectively. The deposition time ( $t_d$ ) was adjusted to 30 min to obtain films with similar thickness in the range of 900–1100 nm.

The atomic concentration profiles of the YbSZ films were measured using two particle accelerators at the Instituto de Física de the Universidad Nacional Autónoma de México. A 3 MV 9SDH-2 NEC Pelletron equipped with a SNICS-II ion source produced a 10.0 MeV  $^{12}\text{C}^{3+}$ , which was used for the HI-RBS technique. A single ended 5.5 MV Van de Graaff (HVECO CN model) produced a 1300 keV  $^2\text{H}^+$  beam to bombard the films in order to measure the O and C concentrations by NRA. The NR  $^{16}\text{O}(d,p_0)^{17}\text{O}$ ,  $^{16}\text{O}(d,p_1)^{17}\text{O}$ ,  $^{16}\text{O}(d,\alpha_0)^{14}\text{N}$  and  $^{12}\text{C}(d,p_0)^{13}\text{C}$  NR peaks in the spectra can be used to measure the O and C if their NR cross sections are well determined. A 500  $\mu\text{m}$  thick surface barrier detector (SBD) equipped with standard electronics set at  $\theta = 165^\circ$  angle was used to measure the particles energy. The incident beams bombarded the samples at  $90^\circ$  angle relative to the target surface. For the  $^2\text{H}^+$  beam experiments, no energy absorbing foil was placed in front of the SBD in order to measure the energies of the NR particles and also the  $^2\text{H}^+$  elastic backscattered energies from the target nuclei. The elastic energies of the  $^2\text{H}^+$  on Si nuclei substrate was used to deduce the total beam particles and the SBD solid angle. These parameters were used for the analysis of the energies spectra. A Gaertner 117A ellipsometer using the 632 nm line from a He–Ne laser was used to measure the refractive index and films thickness. A Siemens D-500 diffractometer was used to perform XRD of the films. This spectrometer used the Cu  $K\alpha 1$  wavelength (1.54056 Å). The incidence angle of the X ray

beam with respect to the film surface was of  $2^\circ$ . The XRD spectra were obtained for  $2\theta$  angles in the range from  $20^\circ$  to  $105^\circ$  with steps of  $0.02^\circ$ .

## 3. Experimental results and discussion

Fig. 1 shows the experimental spectrum (dots) produced by a 1.3 MeV  $^2\text{H}^+$  beam bombardment on the sample YbS1. There are two well-defined regions in the RBS spectrum: (1) the  $^2\text{H}^+$  backscattered on Si nuclei from the film substrate and a peak (60–80 channels) due to the  $^2\text{H}^+$  backscattered from Zr and Yb nuclei. The counting yield from Yb and Zr overlaps to form the peak since this method does not have a good mass separation. However, this method has a good sensitivity to measure the C and O concentrations on the samples through NR. The  $^{16}\text{O}(d,\alpha_0)^{14}\text{N}$ ,  $^{16}\text{O}(d,p_0)^{17}\text{O}$ ,  $^{16}\text{O}(d,p_1)^{17}\text{O}$  and  $^{12}\text{C}(d,p_0)^{13}\text{C}$  NR peaks are indicated in the high energy region of the spectrum. The DataFurnace (DF) code [9] was applied to fit the energy spectra in order to obtain the atomic film profiles. The code fits simultaneously the elastic (RBS) and NR regions of the spectrum (solid line). DF is an automatic fitting code that generates its own layer structure. NR cross sections obtained from the Ion Beam Analysis Nuclear Data Library [IBANDL] were introduced in the DF to obtain the O and C concentrations [10–12]. It may be observed in the Fig. 1 inset the overlapping of the  $^{16}\text{O}(d,\alpha_0)^{14}\text{N}$  and  $^{16}\text{O}(d,p_0)^{17}\text{O}$  NR particle yield, however DF is able to provide the O concentration. The  $^{16}\text{O}(d,p_1)^{17}\text{O}$  NR peak is on top of a pile-up tail of backscattered  $^2\text{H}^+$  deuteron and it was not used because it reduces the accuracy of the NRA measurement. Table 1 shows the atomic O concentrations for the 4 films analyzed. The  $^{12}\text{C}(d,p_0)^{13}\text{C}$  NR peak can be partially attributed to the beam induced

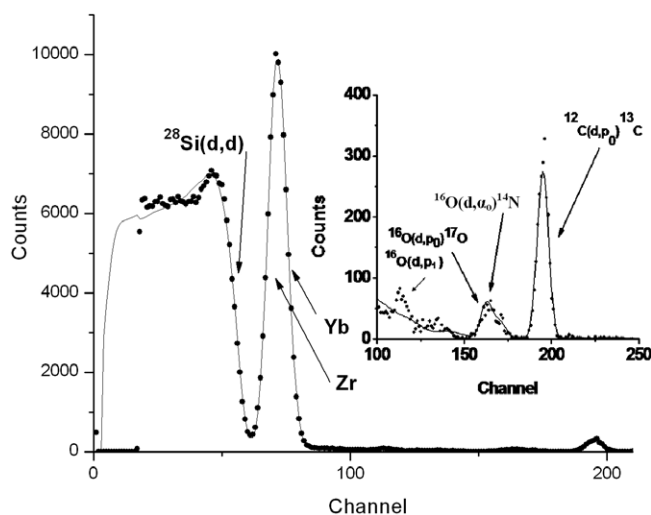


Fig. 1. The figure shows a typical experimental spectrum (dots) produced by a 1300 keV  $^2\text{H}^+$  beam bombardment of the YbS1 sample. The surface barrier detector was set at  $165^\circ$  angle. DataFurnace code (solid line) fitted simultaneously the elastic and NR regions of the spectrum.  $^{16}\text{O}(d,\alpha_0)^{14}\text{N}$ ,  $^{16}\text{O}(d,p_0)^{17}\text{O}$  and  $^{12}\text{C}(d,p_0)^{13}\text{C}$  NR cross section from IBANDL web site were used to fit the NR region of the spectrum.

Table 1

A summary of the Zr, Yb and O atomic concentrations (%) and film thickness of the 4 YbSZ samples doped with different level of  $\text{Yb}_2\text{O}_3$ . The error in the determination of the elements concentrations was estimate to be  $\sim 10\%$ . The films refractive indexes and the grain size are also present

Sample	Mol Yb	Film thickness $10^{15}$ at/cm <sup>2</sup>	O%	Zr%	(Yb/Zr) * 100	Refractive index $n$	Grain size (nm)
YbSZ1	0.0025	1563	65	28	17.8	1.82	5.77
YbSZ2	0.005	1775	66	27	18.5	1.87	5.11
YbSZ3	0.0075	1974	64	28	25.0	2.10	5.01
YbSZ4	0.01	2050	64	26	30.7	2.32	4.94

C build-up during the sample bombardment. Some C is also expected on the films because the use of the  $\text{Yb}(\text{acet})_3(\text{H}_2\text{O})_x$  precursor. The carbon film thickness for the four samples analyzed was in the 90–110 nm range.

Fig. 2 shows a typical HI-RBS experimental spectrum (dots) for the 10.0 MeV  $^{12}\text{C}^{3+}$  beam bombardment of sample YbSZ1. The good depth resolution and excellent mass separation of Yb, Zr and Si can be observed in the spectrum. A backscattered carbon ion from a surface oxygen atom has about 200 keV energy and the signal is on top of the much larger Si spectrum, thus not very useful for measuring the O concentrations. DataFurnace code was also applied to fit the spectrum (solid line) to obtain the atomic film profiles of Yb, Zr and Si. The fitting for Fig. 2 was performed taking into account the O concentrations obtained from the  $^2\text{H}^+$  NRA spectra.

The HI-RBS spectrum shows that the film atomic compositions were homogeneous and the four sample analyzed were obtained with three sublayers: (a) the surface sublayer, providing the film  $\text{Yb}_x\text{Zr}_y\text{O}_z$  stoichiometry and thickness, (b) the interfacial sublayer, providing the  $\text{Si}_x\text{Zr}_y\text{Yb}_z$  composition and thickness and (c) the silicon substrate.

Table 1 summarizes the DataFurnace characterization of the YbSZ films. The refractive indices of the films are also shown in Table 1 and they are in the range from 1.8 to 2.3, which are characteristic of dense metal oxide thin films, such as  $\text{ZrO}_2$ ,  $\text{HfO}_2$ , etc. [13]. As Table 1 shows,

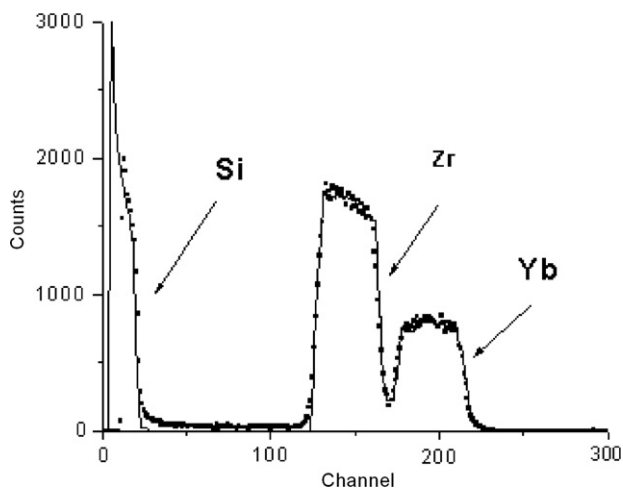


Fig. 2. shows a typical HI-RBS experimental spectrum (dots) for the 10.0 MeV  $^{12}\text{C}^{3+}$  beam bombardment of the same sample YbSZ1 shown in Fig. 1. DataFurnace code (solid line) was used to fit the spectrum: The spectrum fit was done with the prior assumption of the O concentrations obtained from the  $^2\text{H}^+$  NRA.

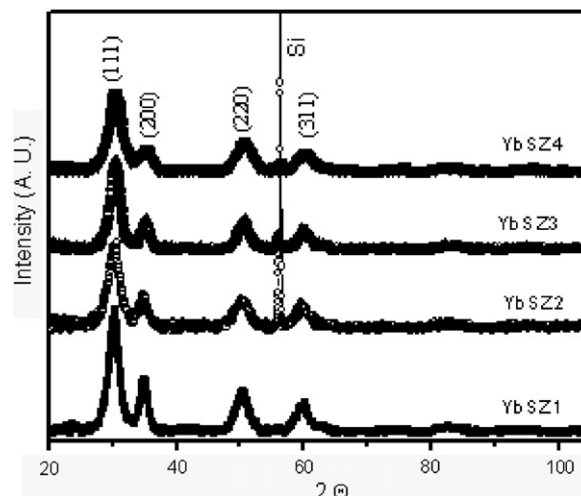


Fig. 3. XRD patterns of the YSZ films prepared by the pyrolysis process using different  $\text{Yb}(\text{acet})_3(\text{H}_2\text{O})_x$  molarities; 0.0025 M (YSZ1), 0.005 M (YSZ2), 0.0075 M (YSZ3) and 0.01 M (YSZ4). The substrate temperature ( $T_s$ ) was kept constant at 425 °C.

the increase in the ytterbia content is consistent with the increase in the refractive index. The fact that the refractive index values of our YbSZ films are higher than those of YbSZ films prepared by the sol-gel approach and annealed at high temperature (1050 °C) [6], indicates that our spray pyrolysis approach favors the formation of denser films.

Fig. 3 shows the typical XRD pattern for the deposited films. These spectra show that all the doped samples have the single phase cubic fluorite structure. The behavior of the full widths at half maximum (FWHM) and intensities of the main (1 1 1) diffraction peak, was such that the grain size calculated by the Voigt function method [14,15], decreases as the Yb increases (see Table 1). This trend in the grain size as a function of the Yb content is similar to that found in YbSZ films prepared by the sol-gel method [6]. We also believe that the extremely small size of the crystalline particles, which is in the nanometer scale, could be responsible for the stability of the cubic phase observed in all our films.

#### 4. Conclusions

The composition and structure of  $\text{ZrO}_2$  thin films doped with different Yb concentrations, prepared by the pyrolysis method have been investigated by ion beam analysis methods, combined with XRD spectroscopy and ellipsometry.

The IBA methods and the XRD patterns measurements, indicate that the Yb atoms in the films are incorporated through the  $\text{Yb}_2\text{O}_3$  phase and that the content of this dopant increases with respect to the increases of the molarity of Yb in the precursor solution.

In consistency with this, the ellipsometry measurements reveal an increase in the refractive index of the films with the Yb content. XRD measurements show that, independently on the Yb content, all the films have the cubic fluorite crystalline phase and that the crystal size, which is in the nanometer scale, decreases as the Yb content increases. It is assumed that the stability of the cubic phase of the crystalline grains is due to their extremely small size.

### Acknowledgements

The authors wish acknowledges to M. en C.E.P. Zavala and K. Lopez for the accelerators maintenance operation. The authors would like to acknowledge the technical assistance of L. Baños, J. Camacho, S. Jimenez and Arcadio Huerta. This work has been partially supported by DGAP-A-UNAM under project IN227807 and CONACyT under project 47303-F.

### References

- [1] J. Will, A. Mitterdofer, C. Kleinlogel, D. Perednis, L.J. Gauckler, *Solid State Ionics* 131 (2000) 79.
- [2] N.Q. Minh, *J. Am. Ceram. Soc.* 76 (1993) 563.
- [3] V. Kozhukharov, N. Brashkova, M. Ivanova, J. Carda, M. Machkova, *Bol. Soc. Esp. Cerám. Vidrio* 41 (2002) 471.
- [4] I. Kosacki, C.M. Rouleau, P.F. Becher, J. Bentley, D.H. Lowndes, *Solid State Ionics* 176 (2005) 1319.
- [5] O. Yamamoto, Y. Arati, Y. Takeda, N. Imanishi, Y. Mizutani, M. Kawai, Y. Nakmura, *Solid State Ionics* 79 (1995) 137.
- [6] A. Hartridge, M.G. Krishna, A.K. Bhattacharya, *Int. J. Mod. Phys. B* 14 (2000) 1017.
- [7] A. Ortiz, J.C. Alonso, E. Haro-Poniatowski, *J. Electron. Mater.* 34 (2005) 150.
- [8] E.B. Ramírez, A. Huanosta, J.P. Sebastian\*, L. Huerta, A. Ortiz, *J.C. Alonso, J. Mater. Sci.* 42 (2007) 901.
- [9] N.P. Barradas, C. Jeynes, R.P. Webb, *Appl. Lett.* 71 (1997) 291.
- [10] H.J. Kim, W.T. Milner, F.K. McGowan, *Nuclear Data Tables v. A3* (1967) 123.
- [11]  $^{16}\text{O}(d,\alpha_0)^{14}\text{N}$ . G. Amsel, *Ann. Phys.* 9 (1964) 297.
- [12] E. Kashy, R.R. Perry, J.R. Risser, *Phys. Rev.* 117 (1960) 1289.
- [13] D. Smith, P. Baumeister, *Appl. Opt.* 18 (1979) 111.
- [14] T.H. Keijser, J.I. Langford, E.J. Mittemeijer, A.B.P. Vogels, *J. Appl. Cryst.* 15 (1982) 308.
- [15] V. Valvoda, X-ray diffraction structure analysis of thin films, in: L. Eckertová, T. Ruzicka (Eds.), *Diagnostics and Applications of Thin Films*, IOP Publishing, London, 1992, p. 115.